Optics Letters

Narrowband silicon waveguide Bragg reflector achieved by highly ordered graphene oxide gratings

YUNG-JR HUNG,[1,3] YA-CHING LIANG,[1] CHIA-WEI HUANG,[1] JYUN-FU SHIH,[1] SHIH HU,[2] TZU-HSIANG YEN,[1] CHIA-WEI KAO,[1] AND CHUN-HU CHEN[2,4]

[1]Department of Photonics, National Sun Yat-sen University, Kaohsiung 80424, Taiwan
[2]Department of Chemistry, National Sun Yat-sen University, Kaohsiung 80424, Taiwan
[3]e-mail: yungjr@mail.nsysu.edu.tw
[4]e-mail: chunhu.chen@mail.nsysu.edu.tw

Received 18 September 2017; revised 14 October 2017; accepted 17 October 2017; posted 19 October 2017 (Doc. ID 307347); published 15 November 2017

Graphene oxide (GO) ultrathin film can be wafer-scale deposited by spin coating, can be patterned by laser interference lithography and oxygen plasma etching, can be thinned atomically (0.26 nm/min) and oxidized by ozone treatment, and is a relatively transparent and low-refractive-index material compared to pristine graphene. All those unique properties prompt us to realize a low-loss (∼5 dB/cm), high-extinction-ratio (19 dB), and narrowband (0.425 nm) GO/silicon hybrid waveguide Bragg reflector by transferring 7-nm-thick GO gratings ($n = 1.58$) atop a silicon strip waveguide. Unlike a sidewall-corrugated strip waveguide Bragg reflector that generally exhibits distorted corrugation profiles and is sensitive to fabrication errors, the as-realized GO-grating-covered strip waveguide Bragg reflector exhibits a stable reflecting wavelength and controllable reflection bandwidth that can be well predicted by numerical simulations. © 2017 Optical Society of America

OCIS codes: (050.2770) Gratings; (230.1480) Bragg reflectors; (230.7370) Waveguides.

https://doi.org/10.1364/OL.42.004768

The implementation of integrated waveguide gratings on a silicon-on-insulator (SOI) substrate to provide a flexible and narrowband spectral response is of vital importance for a wide range of sensing and filtering applications [1–3]. However, due to the small waveguide dimensions for single-mode light propagation in a silicon strip waveguide, any small perturbations on the sidewall corrugations can greatly alter the grating coupling strength and its effective index. This makes it difficult to obtain narrowband reflection from strip silicon waveguide gratings [4,5]. This issue could be mitigated by using a cladding-modulated waveguide grating design on SOI to allow flexible control of the grating coupling strength, thus enabling narrowband reflection [6]. Nevertheless, precise definition of sidewall gratings that are tens of nanometers wide is still challenging by deep ultraviolet (DUV) lithography. The sidewall gratings actually fabricated are severely rounded and distorted, and thus is difficult to control the amplitude and phase of their spectral response [7,8]. Hybrid integration of a thin grating layer made of a transparent and low-index material atop the silicon strip waveguide is an alternative approach to overcome this issue. Graphene oxide (GO) is an oxidized form of 2D graphene material consisting of hydrophilic oxygenated functional groups decorated either on their basal planes or at the edges. Compared to pristine graphene, a controlled quantity of the oxygenated functional groups in GO is advantageous to achieve the desired properties of colloidal stability, transparency, conductivity, catalytic activities, and refractive index [9–12]. Intrinsic negative charges of GO after deprotonation make it capable of being homogeneously dispersed in an aqueous medium for easy device engineering and low environmental impacts, superior to related materials of carbon nanotubes or fullerene-C60. In our previous work, we have developed a reliable chemical oxidation procedure capable of producing significantly oxidized GO capable for large-scale grating [10]. Moreover, the electronic and optical properties of GO can also be chemically reduced to restore its conjugated sp^2-hybridized domains, making it an emerging versatile platform for integrated photonic applications [13].

The complex refractive index of GO is determined by its permittivity and conductivity, which could be changed via voltage modulation and molecule adsorption. Therefore, GO has been widely applied for various sensors combined with a narrowband filter enabled by an optical fiber Bragg grating or a silicon photonic crystal cavity [14,15]. Nevertheless, to our knowledge none of the prior works are focused on the direct patterning of GO thin film into periodic strips to achieve on-chip narrowband reflection. In this Letter, we transfer holographically defined GO gratings onto a silicon strip waveguide to realize a GO/Si hybrid waveguide Bragg reflector that provides a reflection bandwidth of 0.425 nm and an extinction ratio of 19 dB with a low propagation loss of ∼5 dB/cm.

According to the coupled-mode theory, the reflection bandwidth of a grating structure is defined as [16]

$$\Delta\lambda = \frac{\lambda_B^2}{\pi n_g}\sqrt{\kappa^2 + (\pi/L)^2}, \qquad \kappa = \frac{\Gamma(n_1^2 - n_2^2)}{\lambda_0 n_{\mathrm{eff}}}, \tag{1}$$

0146-9592/17/224768-04 Journal © 2017 Optical Society of America

Corrected 17 November 2017

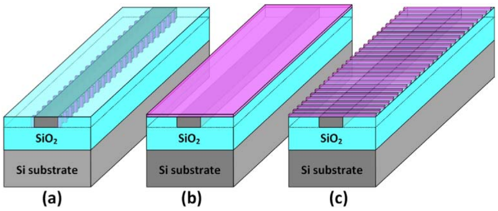

Fig. 1. Schematic diagrams of (a) a sidewall-corrugated silicon strip waveguide grating, (b) a GO-film-covered Si strip waveguide, and (c) a GO-grating-covered silicon strip waveguide grating.

where λ_B, n_g, and L are the Bragg wavelength, the group index, and the total grating length, respectively. Grating coupling strength κ is proportional to the optical overlap factor Γ, the high/low index difference ($\Delta n = n_1 - n_2$), and is inverse proportional to the wavelength in vacuum λ_0 and the effective index n_{eff} of the waveguides. The optical overlap factor is a measure of the fraction of the mode power flux located in the grating region and is calculated using a commercial mode solver FimmWAVE from Photon Design. A fine reflection bandwidth can be obtained by using a long grating structure with a weak grating coupling strength. To achieve this target, a few tens of nanometers corrugation width is typically utilized in sidewall-corrugated strip waveguide gratings, as depicted in Fig. 1(a). In this work, we deposit a thin layer of GO atop a pure silicon strip waveguide, as depicted in Fig. 1(b), to investigate the additional waveguide propagation loss arising from the GO thin film. We also replace the sidewall corrugations on a silicon strip waveguide with a thin GO grating overlay to produce narrowband Bragg reflection on a SOI substrate, as depicted in Fig. 1(c).

The advantages of GO gratings over sidewall corrugations on Si strip waveguides for achieving narrowband reflection are displayed in their respective optical overlap factors shown in Fig. 2. The optical overlap factor to the sidewall corrugations of strip waveguide Bragg reflector is proportional to its corrugation width. Nanometer-scale resolution for the grating definition is therefore required to accurately control the grating coupling strength, which is challenging for the ArF 193-nm lithography widely used for silicon photonics. The rounded sidewall corrugation profiles shown in Fig. 2 reveal the difficulty to precisely control the corrugation width and grating duty cycle. On the other hand, due to the low refractive index of GO material, the optical overlap factor of the GO grating is lower compared to that of the sidewall gratings in strip

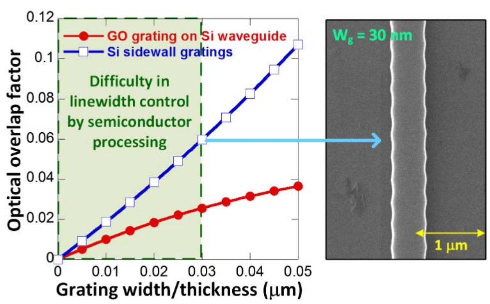

Fig. 2. Calculated optical overlap factors of sidewall-corrugated and GO-grating-covered Si strip waveguide Bragg reflectors, respectively. The figure to the right is the top SEM view of a sidewall-corrugated silicon strip waveguide Bragg reflector with a sidewall corrugation of 30 nm.

waveguides. We also demonstrated that isotropic ozone treatment slows to a 0.26 nm/min etch rate of periodic GO structures, equivalent to ~1/3 of the GO monolayer per minute [10]. This provides flexible and precise thickness determination of the resulting GO gratings. Their x-ray photoelectron spectroscopy (XPS) spectra reveal that the GO material can be further oxidized by post-isotropic ozone treatment. The fraction of the oxygenated carbon in GO is increased from 50.1% to 54.15% after 19 min of ozonation [10].

The fabrication of pure silicon strip waveguides and sidewall-corrugated waveguide Bragg reflectors on SOI were performed at IMEC using a CMOS-compatible process with 193-nm DUV lithography. As-realized 220-nm-thick and 500-nm-wide silicon strip waveguides are sandwiched by a 3-μm-thick bottom thermal oxide cladding, a 220-nm-thick side oxide cladding, and an air top cladding. The height difference between the silicon strip waveguide and side oxide cladding is less than 16 nm. A pair of concentrated surface grating couplers is utilized for optical I/O between the single-mode fiber and silicon strip waveguide with an efficiency of ~38% [6]. The procedures to fabricate GO gratings are disclosed as follows. We utilize a preformed acidic oxidizing medium as a modified Hummers' method for fast and reliable graphite oxidation to generate highly oxidized GO suspension [10]. A thin GO film is deposited on a TiO_2-covered silicon substrate by spin coating. The thickness of the GO film can be controlled by the concentrations of aqueous GO suspension solutions or by post-ozone treatment. After baking, a 70-nm-thick bottom antireflection coating (BARC) layer and a 120-nm-thick positive photoresist layer (AllResist AR-P3170) are sequentially deposited atop the GO film. The samples are then transferred to the laser interference lithography system [17] and exposed to interference fringes with a predefined grating periodicity. Finally, the samples are immersed in a diluted 2.38% tetramethylammonium hydroxide (TMAH) photoresist developer to produce the grating structures. Transferring the resist grating pattern into the GO thin film is conducted by anisotropic oxygen plasma etching to fully etch through the GO film, followed by the removal of residual BARC via isotropic ozone treatment under a lifted temperature of 135°C. After spin-coating a thick polymethyl methacrylate (PMMA) resist atop the GO gratings, the samples are immersed in a buff hydrogen fluoride (HF) solution to etch the underlying TiO_2 layer and to float the PMMA/GO grating film to be transferred onto silicon strip waveguides. The protecting PMMA resist is finally removed by acetone. Figure 3 shows the scanning emission microscope (SEM) and atomic force microscope (AFM) views of an as-realized GO-grating-covered silicon strip waveguide and its Raman spectrum. The well-defined GO gratings sitting atop a silicon strip waveguide have a periodicity of 330 nm and a thickness of 10 nm characterized by AFM. The Raman spectrum reveals that GO gratings still exhibit the signature D (1350–1360 cm^{-1}) and G bands (1592–1608 cm^{-1}), showing that the GO natures can be well preserved after all the fabrication processes [10]. The slightly higher intensity of D to G bands further suggests the high oxidation degrees in the GO grating. The lack of 2D band implicates the destruction of the planar sp^2 carbon network resulting from oxidation of the material [11].

The optical transmission spectra of baseline and GO-film-covered glasses are measured using an UV/VIS spectrophotometer, as shown in the inset of Fig. 4. The propagation loss of

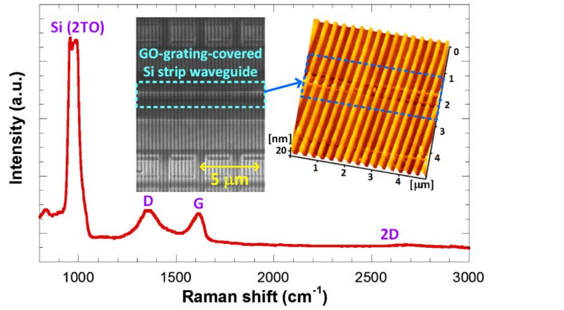

Fig. 3. Raman spectrum and SEM/AFM views of GO-grating-covered silicon strip waveguide Bragg reflector ($P = 330$ nm and $T_{\rm GO} = 10$ nm).

planar, GO-film-covered and GO-grating-covered silicon strip waveguides are measured by the cutback method [18]. About 99.96% optical transmission is observed for a 28-nm-thick planar GO film over the entire C+L wavelength bands under normal incidence. However, when the light propagates in a GO-film-covered silicon strip waveguide, a 28-nm-thick planar GO film atop the silicon strip waveguide produces a huge optical propagation loss of up to 60 dB/cm. Nevertheless, this is still one order of magnitude lower than the propagation loss of silicon strip waveguides covered with a pristine monolayer graphene (~540 dB/cm) [19]. When 28-nm-thick continuous GO film is patterned into periodic strips with a duty cycle of 0.35 and the same thickness, the propagation loss is decreased to 20 dB/cm. The loss can be further reduced by ozone treatment with a rate of around 0.7 dB/cm/min and 0.28 dB/cm/min for GO-film-covered and GO-grating-covered silicon strip waveguides, respectively. This is attributed to the fact that ozone treatment further oxidizes the GO films to decrease the thickness and break down the optical-absorbing pi-conjugation network (C=C) atop the strip waveguide. After 60 min ozone treatment, the propagation loss of the GO-grating-covered silicon strip waveguide is reduced to only 5 dB/cm. Figure 5 shows the measured transmission spectra of sidewall-corrugated and GO-grating-covered silicon strip waveguide Bragg reflectors with different grating widths/thicknesses. The device length of the waveguide Bragg reflectors shown in Fig. 5 is fixed to 0.44 mm.

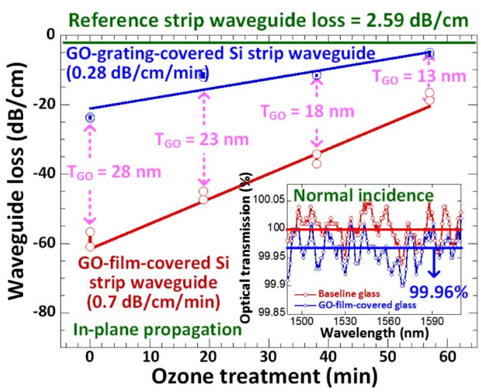

Fig. 4. Measured waveguide in-plane propagation loss of GO-film-covered and GO-grating-covered silicon strip waveguides, respectively, against the ozone treatment time. The inset figure shows the optical transmission spectra of baseline and GO-film-covered glasses, respectively, under normal incidence.

The measured reflection bandwidth of sidewall-corrugated silicon strip waveguide Bragg reflectors ranges from 1.5 to 5.7 nm depending on the grating widths W_g (10–40 nm), corresponding to a grating-width-dependent reflection bandwidth $\delta(\Delta\lambda)/\delta W_g$ of 0.14. With a fixed strip waveguide width, the increase of sidewall grating width leads to the decrease in waveguide effective index. This results in the blueshift of the Bragg wavelength with a rate $\delta(\lambda_B)/\delta(W_g)$ of −0.59, as shown in Fig. 5(a). Note that we obtain a narrower reflection bandwidth from as-fabricated sidewall-corrugated silicon strip waveguide Bragg reflectors than expected in the calculations due to the smoothing of the corrugations caused by the insufficient resolution of DUV lithography. On the other hand, the measured reflection bandwidth of GO-grating-covered silicon strip waveguide Bragg reflector ranges from 0.59 to 1.6 nm depending on the GO grating thickness $T_{\rm GO}$ (13–28 nm), corresponding to a grating-thickness-dependent reflection bandwidth $\delta(\Delta\lambda)/\delta T_{\rm GO}$ of only 0.05. With a fixed strip waveguide width, the increase of GO grating thickness leads to the slight increase of waveguide effective index. This results in the redshift of the Bragg wavelength with a rate $\delta(\lambda_B)/\delta(T_{\rm GO})$ of only 0.06, as shown in Fig. 5(b). The refractive index of GO thin film is characterized to be around 1.58 at 1550 nm of wavelength by spectroscopic ellipsometry (J. A. Woolam, M2000-DI). Figure 5 also reveals that sidewall-corrugated ($W_g = 10$ nm) and GO-grating-covered ($T_{\rm GO} = 28$ nm) silicon strip waveguides have a similar reflection bandwidth, which agrees well with the theoretical prediction in Fig. 2. However, a GO-grating-covered silicon strip waveguide has a lower extinction ratio of only 12 dB due to its high propagation loss of 20 dB/cm, whereas a sidewall-corrugated silicon strip waveguide enables a propagation loss of ~2.8 dB/cm and thus an extinction ratio of 17 dB. An even narrower reflection bandwidth and higher extinction ratio can be pursued by deposing a thinner GO grating on a longer silicon strip waveguide. Since the root-mean-square surface roughness of as-deposited GO film is only 0.59 nm, the thinnest GO grating we have achieved is 4 nm uniformly over the entire 2-in. wafer [10]. In this work we successfully transfer ultrathin GO gratings onto 3.48-mm-long silicon strip waveguides, and their measured transmission spectra are shown in Fig. 6. Only one steep dip exists at the Bragg wavelength of GO-grating-covered silicon strip waveguide Bragg reflectors over the entire 140-nm wavelength range, indicating that

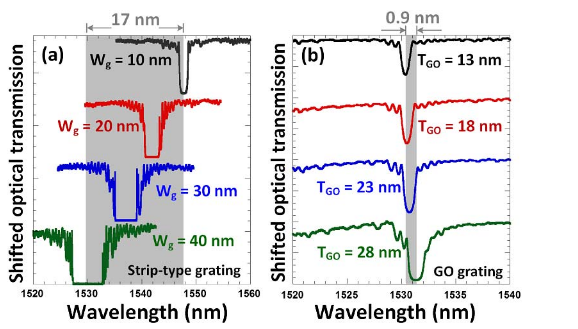

Fig. 5. Measured transmission spectra of (a) sidewall-corrugated Si strip waveguide filters with different grating widths W_g and (b) GO-grating-covered Si strip waveguide filters with different grating thicknesses $T_{\rm GO}$. The device length is 0.44 mm. The grating periodicity is 320 nm. For clarity, the curves are offset in each plot. The vertical scales on (a) and (b) are the same for comparison.

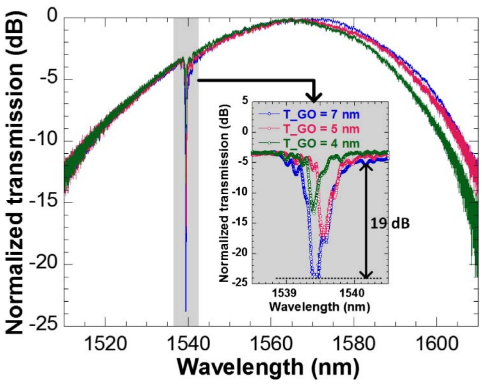

Fig. 6. Measured transmission spectra of GO-grating-covered Si strip waveguide gratings with different grating thicknesses. The device length is 3.48 mm. The grating periodicity is 335 nm.

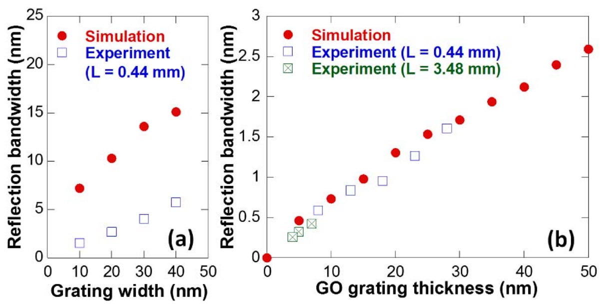

Fig. 7. Simulated and measured reflection bandwidths of (a) sidewall-corrugated and (b) GO-grating-covered silicon strip waveguide Bragg reflectors versus grating width/GO grating thickness.

the higher-order leaky modes can be ignored. Such a sharp dip corresponds to a reflection bandwidth of 0.425 nm and an extinction ratio of 19 dB for the case of 7-nm-thick GO gratings. This corresponds to a grating coupling strength of 23 cm^{-1}. Further reducing the thickness of the GO grating to 4 nm leads to a reflection bandwidth of only 0.26 nm and an equivalent grating coupling strength of 14.2 cm^{-1}. Its low 8-dB extinction ratio indicates the need for an even longer waveguide, but be aware that 500-nm-wide silicon strip waveguide has a phase coherent length of only 4.17 mm [20]. This is attributed to the fabrication nonuniformity that causes fluctuations in waveguide effective index and thus large phase uncertainty. This issue limits the minimum reflection bandwidth achievable in all kinds of waveguide Bragg reflectors on SOI.

Figure 7 shows the simulated and measured reflection bandwidths of sidewall-corrugated and GO-grating-covered silicon strip waveguide Bragg reflectors versus grating width/GO grating thickness. The narrower reflection bandwidth in the as-fabricated devices than simulated values shown in Fig. 7(a) is mainly due to the fact that the simulations were conducted on a square-wave modulation while the actual corrugation profile turned out to be a rounded periodic modulation. The discrepancy between the simulation and experimental results could be substantially reduced by introducing a rounded corrugation profile in the simulation model. On the contrary, depositing well-defined GO gratings atop a silicon strip waveguide enables narrowband reflection with a controllable reflection bandwidth that agrees well with the theoretical predictions based on square-wave modulation.

In summary, the proposed GO/Si hybrid approach leverages from the nature of GO material that enables a transparent, continuous, and ultrathin film by low-cost spin coating. The resulting GO film is patterned into periodic strips by laser interference lithography and anisotropic oxygen plasma and is slowly thinned and oxidized by ozone treatment. By transferring 7-nm-thick and low-refractive-index ($n = 1.58$) GO gratings atop a silicon strip waveguide, the as-realized GO/Si hybrid waveguide Bragg reflector demonstrates a reflection bandwidth of 0.425 nm and an extinction ratio of 19 dB. For practical applications, wafer-scale definition of GO gratings can be conducted directly on top of silicon waveguides without requiring a film transfer process, and thus is compatible with the existing semiconductor manufacturing processes. We anticipate that the proposed GO/Si hybrid waveguide filter is promising for not only a variety of sensor applications but also the applications that utilize gratings for on-chip signal processing and photonic generation of arbitrary microwave waveforms [21].

Funding. Ministry of Science and Technology, Taiwan (MOST) (103-2221-E-110-038, 104-2221-E-110-061, 105-2221-E-110-075); Industrial Technology Research Institute (ITRI).

REFERENCES

1. M. W. Puckett, F. Vallini, A. Grieco, and Y. Fainman, Opt. Lett. **40**, 379 (2015).
2. Y.-J. Hung, C.-J. Wu, T.-H. Chen, T.-H. Yen, and Y.-C. Liang, J. Lightwave Technol. **34**, 4329 (2016).
3. N. N. Klimov, S. Mittal, M. Berger, and Z. Ahmed, Opt. Lett. **40**, 3934 (2015).
4. X. Wang, W. Shi, H. Yun, S. Grist, N. A. F. Jaeger, and L. Chrostowski, Opt. Express **20**, 15547 (2012).
5. H.-C. Kim, K. Ikeda, and Y. Fainman, Opt. Lett. **32**, 539 (2007).
6. Y.-J. Hung, K.-H. Lin, C.-J. Wu, C.-Y. Wang, and Y.-J. Chen, IEEE J. Sel. Top. Quantum Electron. **22**, 4402507 (2016).
7. A. D. Simard, N. Belhadj, Y. Painchaud, and S. LaRochelle, IEEE Photon. Technol. Lett. **24**, 1033 (2012).
8. A. D. Simard, N. Ayotte, Y. Painchaud, S. Bedard, and S. LaRochelle, J. Lightwave Technol. **29**, 3693 (2011).
9. A. M. Dimiev and S. Eigler, *Graphene Oxide: Fundamentals and Applications* (Wiley, 2016).
10. C.-H. Chen, S. Hu, J.-F. Shih, C.-Y. Yang, Y.-W. Luo, R.-H. Jhang, C.-M. Chiang, and Y.-J. Hung, Sci. Rep. **7**, 3908 (2017).
11. C.-C. Kuo and C.-H. Chen, Nanoscale **6**, 12805 (2014).
12. W.-Y. Kao, W.-Q. Chen, Y.-H. Chiu, Y.-H. Ho, and C.-H. Chen, Sci. Rep. **6**, 37174 (2016).
13. K. P. Loh, Q. Bao, G. Eda, and M. Chhowalla, Nat. Chem. **2**, 1015 (2010).
14. S. Sridevi, K. S. Vasu, S. Asokan, and A. K. Sood, Opt. Lett. **41**, 2604 (2016).
15. X. Gan, C. Zhao, Q. Yuan, L. Fang, Y. Li, J. Yin, X. Ma, and J. Zhao, Appl. Phys. Lett. **110**, 151107 (2017).
16. H. A. Haus and R. V. Schmidt, Appl. Opt. **15**, 774 (1976).
17. Y.-J. Hung, H.-J. Chang, P.-C. Chang, J.-J. Lin, and T.-C. Kao, J. Vac. Sci. Technol. B **35**, 030601 (2017).
18. D. B. Keck and R. Tynes, Appl. Opt. **11**, 1502 (1972).
19. L. A. Shiramin, A. Bazin, S. Verstuyft, S. Lycke, P. Vandenabeele, G. Roelkens, and D. Van Thourhout, in *Conference on Lasers and Electro-Optics (CLEO)* (2017), paper SW4K.6.
20. Y. Yang, Y. Ma, H. Guan, Y. Liu, S. Danziger, S. Ocheltree, K. Bergman, T. Baehr-Jones, and M. Hochberg, Opt. Express **23**, 16890 (2015).
21. L. R. Chen, J. Lightwave Technol. **35**, 824 (2017).

140.117.31.42 {ts '2017-11-28 21:20:28'}